Environmental Earth Sciences (2023) 82:144
https://doi.org/10.1007/s12665-023-10816-3

ORIGINAL ARTICLE

Hydrogeochemical characterization of the alluvial aquifer of Catania Plain, Sicily (South Italy)

S. Morici[1] · E. Gagliano Candela[1] · R. Favara[1] · L. La Pica[1] · C. Scaletta[1] · G. Pecoraino[1]

Received: 26 September 2022 / Accepted: 18 February 2023

Abstract

A hydrogeochemical study was carried out on the shallow Catania Plain alluvial aquifer, in eastern Sicily to reconstruct its hydrogeological structure, the meteoric recharge and to assess the influence of human activities on groundwater. To characterize the geochemistry of the shallow aquifer, two sampling campaigns were carried out, August–October 2004 and April–May 2005 in 47 sites distributed throughout the plain. The samples were collected and analyzed for physical–chemical parameters and major ions, as well as stable isotopes ($\delta^{18}O$ and $\delta^{2}H$). Alluvial deposits with heterogeneous grain sizes constitute the aquifer. Varying conditions of vertical and horizontal permeability lead to the presence of a multilayered aquifer with different conditions of confinement and partial interconnection among layers. The sampled waters were separated into four groups of different compositions due to the water–rock interaction with the different lithologies present in and around the study area. Maps of electrical conductivity and sulfate show a systematic control of land use, in correspondence with the biggest farms. High sulfate concentration is due to both the natural interaction between local meteoric waters and Etna's plume and the mixing with groundwater coming from the area where evaporitic rocks of the Gessoso Solfifera formation are present. In addition, anthropogenic contamination cannot be ruled out. A rain gauge network, consisting of 3 sites located at different altitudes, was installed to collect rain waters to determine isotopic data ($\delta^{2}H$ and $\delta^{18}O$) and to measure the monthly rainfall amount. Based on the isotopic composition of sampled waters, it has been established that beyond the direct meteoric recharge, the recharging areas are in the North (Mt. Etna) and the South (Hyblean Plateau).

Keywords Hydrochemistry · Stable isotopes · Hydrogeology · Catania plain

Introduction

Catania Plain (CP) is an alluvial plain located in eastern Sicily (Fig. 1) with an area of about 430 km^2. Mt Etna borders it to the North, the Ionian Sea to the East, the Hyblean Plateau to the South and the Erei Mts to the West-Northwest. The CP is constituted by recent and present Simeto River and its tributaries (Dittaino and Gornalunga) fluvial deposits. The thick alluvial deposits are interrupted to the South by calcareous and igneous reliefs of the Hyblean Plateau.

The most important economic activities are factories and agriculture (mainly citrus orchards, and animal husbandry). During the last 50 years, urban and industrial development has led to a sharp increase in the demand for water resources in Italy, which, in turn, has led to a rise in the exploitation of groundwater located in alluvial aquifers (Capaccioni et al. 2005). In the CP, irrigation is provided by the presence of rivers, irrigation canals and hundreds of wells.

Many studies exist about CP hydrogeology (Ferrara and Marchese 1977; Ferrara 1979, 1998, 1999; Ferrara and Pappalardo 2004; Guastaldi et al. 2014) and institutional researches were funded (Cassa per il Mezzogiorno 1982; Regione Siciliana-INGV 2005). Nowadays, few studies exist on the geochemical characterization of groundwater. Furthermore, the published papers have been based on data taken in very small areas (few km^2) near factories, agricultural and industrial areas and/or in a few wells (Battaglia et al. 1991; Capaccioni et al. 2005).

This work aims to carry out a hydrogeochemical characterization of the CP shallowest alluvial groundwater, to detect water–rock interaction processes and the presence of anthropogenic pollutants.

✉ S. Morici
sabina.morici@ingv.it

[1] Istituto Nazionale di Geofisica e Vulcanologia, Sezione di Palermo, Via Ugo La Malfa 153, 90146 Palermo, Italy

Published online: 10 March 2023

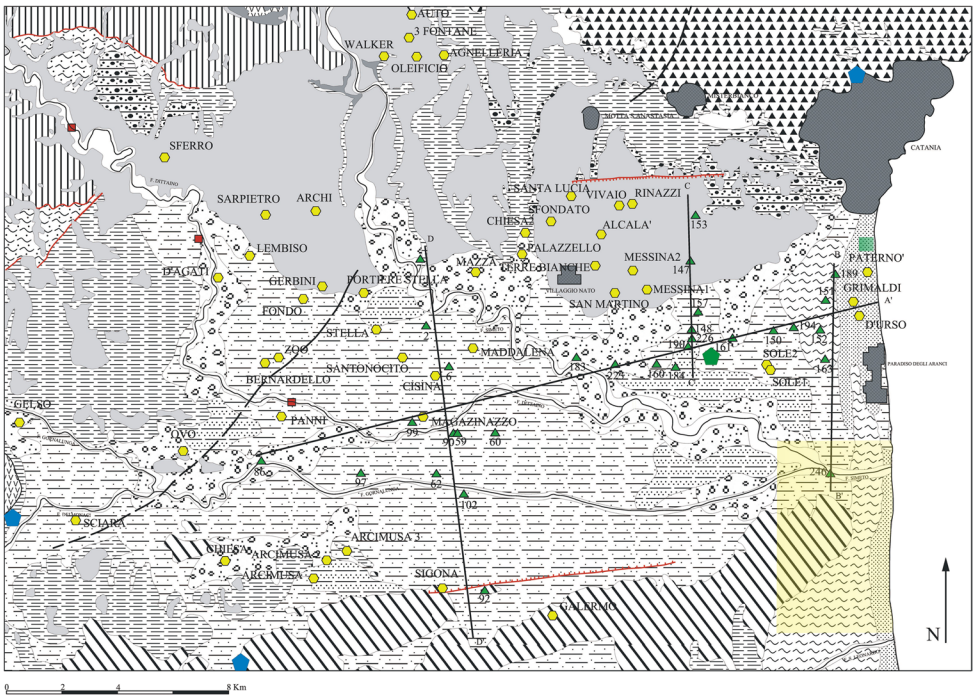

LEGEND

- Alluvium (Holocene)
- Sands and coastal dunes (Holocene)
- Silts (Holocene)
- Recent alluvial deposits (Holocene)
  - a: Silty clay - sandy clay
  - b: Clay sandy
  - c: Sands and gravels
- Contiental and marine terraced alluviums (Tyrrhenian - Holocene)
- Etnean vulcanites (Upper Pleistocene - Holocene)
- Sandy clay
  - 1: Sands, sandstones, conglomerates (mid-Pleistocene)
  - 2: Blue marly clays (Lower Pleistocene)
- Gypsum, “calcari di base”, tripoli and “argille brecciate” (Messinian)
- Terravecchia: clays with sandstone intercalations (Tortonian)
- Flysch Numidico (Lower Miocene)
- Monte Judica: marly clays with levels of glauconitic sandstones (Upper Oligocene - mid-Miocene)
- Sequence Iblea: calcarenites e volcanites (Oligocene - Quaternary)
- Investigated area (Battaglia et al. 1994)
- Investigated area (Capaccioni et al. 2005)
- Rain gauge
- Pheatimeter Iunghetto
- Fault
- Tectonic contact
- Gela thrust
- Wells with stratigraphy
- Sampled water
- River Dittaino sampling points
- Urban centers
- Traces of cross-section

Fig. 1 Simplified geological map of the Catania plain. The yellow square represents the investigated area by Battaglia et al. (1994), and the light green square represents the investigated area by Capaccioni et al. (2005)

In addition, through water isotopic data (δ^2H and $\delta^{18}O$), it was possible to identify possible recharge areas and related hydrologic circuits, allowing to protect them from potential sources of pollution in an attempt to preserve the quality of the water supply. Geological, hydrological and geophysical (Vertical Electrical Surveys) data as well as stratigraphic data from deep and shallow wells have been re-interpreted to redraw the hydrogeological structure of the alluvial aquifer. Finally, in an attempt to estimate the recharge time, the correlation between rainfall and groundwater level was investigated.

The geochemical characterization of the study area was determined based on sampling campaigns carried out between 2004 and 2005. These data may be useful to study the geochemical variations in the CP aquifer almost two decades later to understand the impact of climatic variations in the Mediterranean area on water resource quality.

Geological and hydrogeological settings

The CP is located (Fig. 2) in the foredeep area originating from the collapse of the North-Western and Northern parts of the Hyblean foreland dipping under the most external Appeninic-Maghrebian chain thrust (Lentini 1982). In this geodynamic contest, since about 600 ka the active volcanic system of Mt. Etna has developed north of the CP. The plain is bounded to the East by 300 km, NNW–SSE trending Hyblean-Maltese continental slope (Torelli et al. 1998).

The CP consists of the deposits of the three main rivers that cross it in the W–E direction: Simeto, Dittaino and Gornalunga. These deposits are formed by a Middle–Upper Pleistocene foredeep sequence:

- Marine blue marly clays, outcrop near the towns of Catania, Paternò, Fiumefreddo and Vena (Lower-middle Pleistocene);
- Sandstones and gravels belonging to S. Giorgio Formation, outcrop to West of Catania town (Middle Pleistocene);
- Gravel and conglomerates, Mt. Tiritì Formation, South of Misterbianco and Paternò (Terreforti Hills) (Middle-Upper Pleistocene)
- Marine, deltaic and alluvial deposits (fine sands, silts and grey muds with gravel) of the Simeto River, southern sector of CP (Holocene-Present).

To the North, ancient alluvial terraces, constituted by the alternation of more or less coarse clays and sands, probably originated by the flowing of torrential apparatus coming from Mt Etna, bound the CP.

To the South, the plain is bordered by hills constituted mainly by tuffs, breccia and basalts (originated by the Mt Lauro volcanic activity), locally covered by arenaceous limestones, and as a whole covered by recent CP clays. To the West and North-West, hill relief is constituted by the

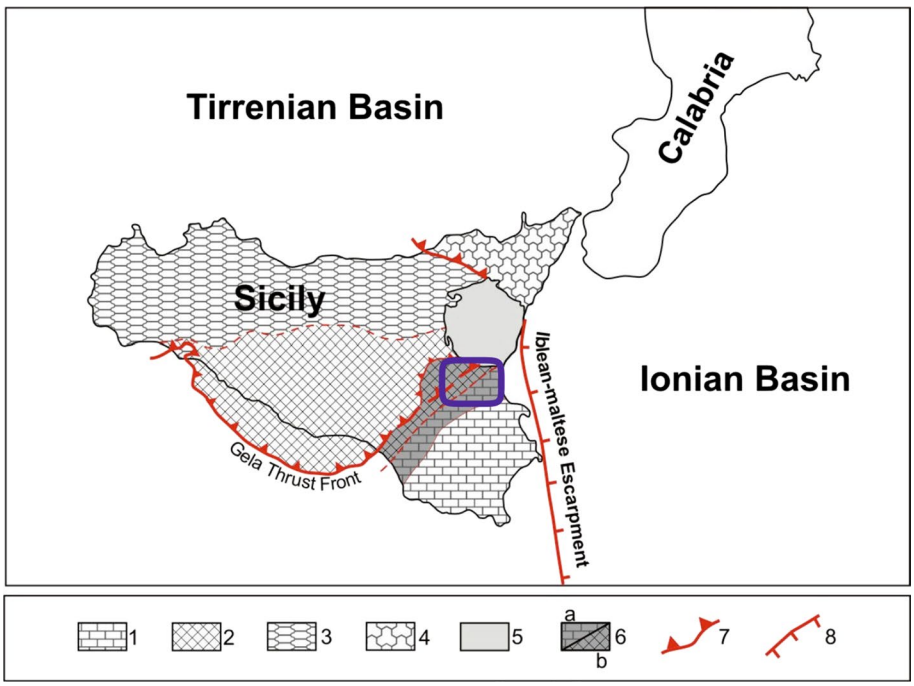

Fig. 2 Tectonic sketch map of Sicily (redraw from Catalano et al. 2000, 2004): (1) Pelagian Block (Hyblean foreland); (2) Gela thrust wedge; (3) Appeninic-Maghrebian thrust belt units; (4) Calabrian arc units; (5) Mount Etna vulcanites; (6) Gela-Catania foredeep deposits: **a** Middle–Upper Pleistocene deposits on allochthonous units. **b** Quaternary deposits on the Hyblean sequences; (7) main thrust fronts; (8) normal faults. The blue square is the study area

Gessoso Solfifera evaporitic sequence (Tripoli-Calcari di Base-Gessi, Grasso and Manna 1990) and Miocene clays (Fig. 1) borders the CP.

Alluvial deposits constitute the CP aquifer with heterogeneous granulometry partially interconnected due to varying vertical and horizontal permeability that lead to the presence of multilayered aquifers with different conditions of confinement. The highly variable horizontal and vertical porosity, permeability (5×10^{-2} to 10^{-4} m/s) and transmissivity (1×10^{-3} to 5×10^{-3} m^2/s) influence the water flow inside the aquifer (Ferrara 1999; Ferrara and Pappalardo 2004).

Sampling and analytical methods

To characterize the shallow aquifer, 47 sites, distributed over the whole plain, have been sampled in the period August–October 2004. From April to May 2005, 41 of them have been re-sampled. Many wells have a diameter lower than 1 m and a maximum depth of 35 m. Three samples along the Dittaino River have been sampled for comparison (Fig. 1). Temperature, pH, electric conductivity (EC), and Eh of sampled waters were measured directly in the field by Orion 150 (EC, T) and 205 (pH and Eh) portable instruments and specific electrodes. The alkalinity was determined by titration with HCl 0.1 N in the laboratory. Water samples were collected and stored in a low-density polyethene flask. Major constituents were analyzed using a DIONEX DX 120 ion chromatograph, on separate unfiltered and un-acidified (Cl^-, NO_3^- and SO_4^{2-}) and filtered (0.45 µm), acidified (Na^+, K^+, Mg^{2+} and Ca^{2+}) sample aliquots. Analytical precision was always better than ± 3%. A Dionex CS-12A column was used for the determination of cations and a Dionex AS14A column for anions.

A rain gauge network, consisting of three sites located at different altitudes (0–285 m asl), was monthly collected. The rain gauges were bulk samplers and the collectors were filled with pure mineral oil to form a film of about 5 mm thickness to avoid water evaporation.

Rainwater and groundwater samples were analyzed for their oxygen and hydrogen isotopic composition, using Analytical Precision AP 2003 and FinniganMAT Delta Plus spectrometers, respectively. The isotope ratios are expressed as the deviation per mille (δ‰) from the reference VSMOW standard. The uncertainties are ± 0.1‰ for $\delta^{18}O$ and ± 1‰ for δ^2H (one standard deviation).

Table 1 reports the chemical composition of the major component. Tables 3 and 4 report the values of $\delta^{18}O$ and δ^2H of rainwater and groundwater.

Results and discussion

Hydrogeology

In this work, with the support of re-analyzed stratigraphy of deep wells and Vertical Electrical Sounding (VES) (Fig. 3a–d; Breusse and Huot 1954; Cassa per il Mezzogiorno 1982), and in agreement with Ferrara and Pappalardo (2004), three different interposed aquifers, sometimes interconnected with each other both vertically and horizontally, have been recognized, according to the following hydrogeological scheme (Table 2):

- A shallow unconfined aquifer, 3–35 m in thickness, in present and recent alluvial deposits and in continental and marine alluvial terraces. The water table is a few meters in depth.
- An intermediate semi-confined aquifer, 3–43 m thick, constituted by clayey–sandy layers, sand and sandy-gravels levels belonging to recent alluvial deposits. The water level is at about 13–15 m depth (Ferrara 1999; Capaccioni et al. 2005).
- A deep semi-confined aquifer with a 20 m maximum thickness constituted by sands, sandstones and conglomerates of Medium Pleistocene age. The water level is at about 30–40 m depth (Ferrara 1999; Capaccioni et al. 2005).

Vertical and horizontal interconnections among these aquifers are recognizable mainly in the southern area (Fig. 3b–d). The existence of other aquifers, isolated or hydraulically interconnected with the main aquifers, cannot be excluded. The aquifer system is fed by local meteoric waters, by rivers crossing the plain and by recent and ancient streambeds coming down from neighboring hills (Ferrara 1999).

The main direction of groundwater flow in the plain is W–E along the hydrographic network (Ferrara 1999). To the North, close to Mt Etna, the shallower aquifer consists of marine and continental alluvial terraces in hydraulic connection with the Etnean aquifer and the intermediate and deep alluvial aquifers (Fig. 3; Ferrara 1999; Capaccioni et al. 2005).

In this study, the stratigraphic data of a large number of drilled wells, most of which reach the lower confining clayey bed, and the data deriving from geophysical surveys (VES) were correlated (Breusse and Huot 1954; Cassa per il Mezzogiorno 1982) for the elaboration of the stratigraphic sections in Fig. 3. In particular, the section of Fig. 3a highlights the morphology of the top of the lower confining clayey bed characterized by many depressions roughly trending

Table 1 Descriptive of the physicochemical parameters and major ions of the groundwater ($N=88$) and surface water ($N=3$; Dittaino river)

Sample	Id	Latitude N UTM	Longitude E UTM	Date	Tw (°C)	Eh (mV)	pH	EC (µS/cm)	Ca^{2+} (meq/l)	Mg^{2+} (meq/l)	K^{+} (meq/l)	Na^{+} (meq/l)	Cl^{-} (meq/l)	NO_3^{-} (meq/l)	SO_4^{2-} (meq/l)	HCO_3^{-} (meq/l)
3 Fontane	1	4,154,750	490,800	I	20.2	158.9	7.18	1451	4.59	7.41	0.61	8.2	3.9	0.9	2.93	12.8
Agnelleria	2	4,154,362	492,082	I	22	78	6.95	2576	12.04	6.74	0.05	19.12	13.06	2.17	14.06	9
				II	17.3	108.5	7.15	3949	13.24	8.26	0.09	24.41	16.7	2.09	18.37	8.6
Alcalà	3	4,147,758	497,832	I	19.2	270	6.83	1659	9.84	4.27	0.25	5.35	6.77	1.44	3.4	8.3
				II	19.5	188.5	6.83	1846	11.45	5.12	0.25	5.87	8.09	2.02	3.97	8.5
Archi	4	4,148,794	487,377	I	22	133	7	3225	19.14	7.49	0.34	20.75	21.81	3	17.58	5.65
				II	18	140.4	7.11	4175	21.86	9.19	0.12	21.55	25.1	3.36	18.37	5.5
Arcimusa	5	4,135,545	487,358	I	18.5	165	7.21	2924	15.8	14.94	0.21	8.49	18.12	2.68	12.84	6.1
				II	17.5	225.4	7.3	3062	15.8	15.29	0.2	8.36	17.69	3.26	11.8	5.95
Arcimusa 2	6	4,136,232	487,852	I	18.5	287.9	7.13	2605	11.32	11.62	0.16	15.11	17.69	2.65	10.22	7.2
				II	18.4	180.9	7.04	2710	9.12	9.48	0.14	12.34	13.2	2.11	7.35	7.55
Arcimusa 3	7	4,136,515	488,557	I	21.3	258.1	7.17	2731	11.24	12.33	0.26	15.23	20.24	1.49	10.24	6.8
				II	18.9	265.2	7.14	3126	8.89	10.64	0.27	16.8	15.88	3.02	10.82	6.9
Auto	8	4,155,821	490,883	I	20.1	158.6	7.75	1230	4.32	8.08	0.56	6	2.24	0.67	1.72	14.3
				II	20.6	106.1	7.75	1557	4.33	7.66	0.53	6.24	2.29	0.72	1.76	14.1
Bernardello	9	4,143,263	485,615	I	22	40.2	6.9	10,571	36.56	38.68	3.26	90.49	76.93	0.01	74.21	13.5
				II	15	142.7	7.39	8843	33.29	31.02	1.71	67.84	57.49	0.61	66.08	9.9
Chiesa	10	4,136,171	484,203	I	20.7	217.2	7.26	3066	17.94	11.22	0.23	6.47	16.04	2.8	11.74	5.4
				II	19.3	94	7.16	3227	19.4	12.47	0.13	6.86	16.89	2.56	13.91	5.35
Chiesa 2	11	4,147,625	494,752	I	22.8	215	7.23	2503	10.19	7.33	0.29	13.38	10.71	1.57	10.66	8.15
				II	21.5	−45.2	7.05	2927	11.65	8.15	0.32	14.28	14.33	0.01	11.88	8.5
Cisina	12	4,142,753	491,807	I	19.7	228	7.04	2991	12.84	10.11	0.44	15.72	15.45	0.58	16.75	7.1
				II	19.9	164	7.03	2940	12.13	9.69	0.41	14.72	13.82	0.55	15.01	7.2
D'Agati	13	4,146,341	483,897	I	19.6	100.7	6.88	10,000	30.97	30.23	5.34	69.4	61.52	6.05	62.14	8.6
D'Urso	14	4,144,968	507,055	I	23.6	153.3	7.21	3859	17.48	9.31	1.4	23.37	32.44	3.59	11.01	4.35
				II	20.4	69	7.41	3863	17.33	9.33	1.31	21.88	30.06	3.34	10.51	4.55
Fondo	15	4,145,577	486,974	I	20.1	195	7.7	3376	15.49	10.19	1.65	19.48	17.6	0.47	20.24	7.5
				II	14.8	99.8	7.36	3821	16.93	11.4	1.56	21.14	21.34	0.82	21.04	7.55
Galermo	16	4,134,221	495,973	I	19.8	153.6	7.3	2833	11.42	13.74	0.58	8.45	17.91	8.15	4.88	4.1
				II	19.5	177.4	7.19	2530	12.55	10.01	0.49	6.98	11.48	7.17	3.77	7.1
Gelso	17	4,141,151	476,766	I	18.8	122.5	6.7	6629	33.36	18.47	0.5	31.75	35.84	3.27	36.08	8.1
				II	18.2	88.6	6.98	6380	32.28	19.14	0.5	31.36	35.48	3.92	34.8	7.4
Gerbini	18	4,146,039	487,687	I	18.5	159	6.8	2895	15.89	7.07	0.1	15.06	16.5	1.37	14.66	6.7
				II	17.2	222.6	6.9	3439	17	8.11	0.09	15.1	17.37	1.71	14.67	6.5
Grimaldi	19	4,145,513	506,813	I	24.6	144.5	7.49	2000	9.97	5.6	0.93	8.94	10.46	2	8.94	4.1
				II	17.6	217.7	7.6	1982	10.26	5.52	0.92	9.04	9.79	2.17	8.55	4.5

Table 1 (continued)

Sample	Id	Latitude N UTM	Longitude E UTM	Date	Tw (°C)	Eh (mV)	pH	EC (µS/cm)	Ca^{2+} (meq/l)	Mg^{2+} (meq/l)	K^{+} (meq/l)	Na^{+} (meq/l)	Cl^{-} (meq/l)	NO_3^{-} (meq/l)	SO_4^{2-} (meq/l)	HCO_3^{-} (meq/l)
Lembiso	20	4,147,130	485,099	I	18.5	120.7	7.16	3866	20.98	11.61	1.01	23.05	26.64	1.98	22.95	5.7
				II	18.7	146.6	7.03	4648	23.31	12.87	1.07	24.3	28.41	2.45	24.43	6
Maddalena	21	4,143,821	493,119	I	18.9	−50.9	7.17	2598	10.8	12.09	0.7	12.64	12.88	0.01	13.27	10.35
				II	18.8	147.7	7.23	2679	10.26	11.05	0.63	12.32	12.3	0.01	12.4	9.15
Magazinazzo	22	4,141,083	491,277	I	20	148	7.8	8590	23.58	31.95	1.67	64.25	60.9	0.01	52.83	7.5
				II	15.8	213	7.55	7449	23.48	27.98	1.42	54.06	48.17	2.49	48.1	7.4
Mazza	23	4,146,621	493,165	I	21.2	275	6.93	2803	12.74	7.41	0.33	15.21	13.71	1.65	12.72	7.4
				II	18.4	316	6.98	2778	12.57	7.67	0.34	15.18	13.54	1.7	12.81	7.3
Messina1	24	4,145,925	499,390	I	19.7	175.3	6.81	1559	8.62	3.51	0.31	5.79	5.74	0.71	3.22	8.75
				II	19	103.2	6.87	1486	9.59	3.84	0.3	5.88	5.87	0.84	3.4	9.25
Messina2	25	4,146,630	498,895	I	20.1	176.3	6.9	1769	9.58	4.82	0.21	6.41	7.14	0.91	4.27	8.75
				II	18.4	137.3	7.04	1713	10.31	5.19	0.21	6.64	7.5	1.11	4.62	8.7
Oleificio	26	4,154,284	491,075	I	27	82.9	7.11	2858	10.48	9.97	0.4	21.6	25.5	1.53	8.84	7.75
				II	22.9	−9.8	7.22	3586	9.87	9.46	0.27	21.19	22.97	1.56	10.15	6.8
Ovo	27	4,140,084	482,661	I	23.6	152	7.7	2070	7.45	4.67	0.21	12.71	11.84	0.73	8.11	4.5
				II	16.5	211.9	7.81	2018	7.42	5.06	0.17	12.75	10.98	0.76	7.84	5.1
Palazzello	28	4,146,945	494,662	I	19.9	218	7.11	2799	14.65	7.96	0.34	12.88	13.23	2.33	12.52	6.9
				II	18.9	162.8	7.09	2744	13.83	7.46	0.32	13.13	13.08	2.1	12.63	6.65
Panni	29	4,141,371	486,202	I	24.6	−39.1	7.29	5387	23.02	17.01	0.38	37.81	33.27	0.01	34.78	9.05
				II	19.5	10.3	7.14	4818	20.29	14.42	0.55	29.17	26.01	0.42	30.41	8
Paternò	30	4,146,548	507,345	I	21.1	140.1	7.41	1364	5.96	3.29	0.61	6.19	6.6	1.09	3.67	4.5
				II	18.7	31.8	7.49	1407	6.01	3.78	0.63	6.17	6.15	0.91	4.3	4.9
P. Stella	31	4,145,762	489,163	I	19.4	144.7	7	2780	12.02	7.02	0.29	15.65	13	1.59	14.34	6.2
				II	17.5	217.3	7.03	2675	12.7	7.83	0.18	15.53	13.48	1.87	13.99	6.45
Rinazzi	32	4,148,977	498,896	I	20.5	189	6.97	1602	11.5	3.26	0.08	4.16	7.05	1.61	4.27	6.3
San Martino	33	4,145,857	498,243	I	21	273	7	1480	10.43	2.35	0.21	4.57	6.44	1.09	4.9	5.35
				II	20.1	275.1	6.97	1560	11.04	2.45	0.24	4.88	6.75	1.22	5.14	5.45
Santa Lucia	34	4,148,973	496,928	I	19.7	249.3	6.87	2047	12.9	4.18	1.32	5.26	9.18	3.04	4.78	6.65
				II	19	169.5	6.99	1844	11.51	3.95	1.37	5.03	8.18	2.29	4.53	6.85
Santonocito	35	4,143,502	490,566	I	19.4	198	6.87	2947	12.99	9.82	0.47	13.65	14.04	1.45	15.08	6.5
				II	19.2	165.1	7.03	3023	13.2	10.04	0.48	13.6	14.19	1.65	15.45	6.4
Sarpietro	36	4,148,636	485,570	I	28	79.6	7.05	3040	17.1	7.35	0.26	15.62	19.22	2.06	14.79	4.8
				II	18.9	66.8	7	4312	20.94	9.72	0.11	19.17	24.24	2.71	17.73	4.8
Sciara	37	4,137,604	478,780	I	20.2	233.3	7.33	3769	17.18	16.91	0.23	19.66	21.5	2.27	22.3	8.85
				II	20.1	94.3	6.92	3920	17.84	17.53	0.22	19.04	20.06	2.05	22.6	9.4

Table 1 (continued)

Sample	Id	Latitude N UTM	Longitude E UTM	Date	Tw (°C)	Eh (mV)	pH	EC (µS/cm)	Ca^{2+} (meq/l)	Mg^{2+} (meq/l)	K^{+} (meq/l)	Na^{+} (meq/l)	Cl^{-} (meq/l)	NO_3^{-} (meq/l)	SO_4^{2-} (meq/l)	HCO_3^{-} (meq/l)
Sferro	38	4,150,684	482,008	I	22.7	178.8	7.13	2870	11.38	6.5	0.53	16.39	15.75	2.6	12.61	4.75
				II	17.8	101.2	7.09	3317	15.8	9.22	0.57	17.2	19.7	2.78	14.01	5
Sfondato	39	4,148,392	495,884	I	19.5	213	7.22	1162	7.98	2.15	0.06	5.99	6.12	0.54	4.82	4.5
Sigona	40	4,135,217	491,989	I	24.9	218.6	7.89	1949	2.32	7.86	0.47	10.39	15.97	0.23	2.75	2.65
				II	23.8	99	7.92	2028	2.65	8.02	0.49	10.39	15.28	0.23	2.67	3.2
Sole1	41	4,143,093	503,789	I	20	−84.7	7.37	1786	5.37	3.94	0.16	8.28	10.09	0.01	1.32	6.4
				II	19.9	−78.9	7.33	1477	5.66	4.16	0.18	8.09	10.02	0.01	1.25	6.65
Sole2	42	4,143,209	503,722	I	20.7	−63.6	7.45	1209	4.8	2.95	0.14	4.66	4.3	0.01	1.46	6.9
				II	20.2	−46.2	7.31	1009	5.04	3.13	0.15	4.59	4.24	0.01	1.46	7.45
Stella	43	4,144,494	489,617	I	19.4	217.3	7.05	2026	9.66	4.72	0.12	11.12	8.79	1.08	8.6	6.75
T. Bianche	44	4,146,775	497,498	I	33.5	149	6.89	1596	10.52	2.86	0.09	5.44	7.42	1.32	4.78	5.5
Vivaio	45	4,148,965	498,867	I	20.6	173.4	7.03	1041	6.67	2.87	0.19	3	3.67	0.62	2.45	6.1
				II	19	51.8	7.01	1240	8.72	3.42	0.15	3.19	4.93	1.17	2.73	6.3
Walker	46	4,154,312	489,906	I	19.4	149	7.27	1725	3.44	8.56	0.51	8.68	3.05	1.02	2.55	14.3
				II	18.9	114	7.36	1780	3.8	8.63	0.5	8.54	3	1.05	2.56	14.25
Zoo	47	4,143,511	486,120	I	20	−36	6.74	8856	34.14	27.83	0.76	63.92	61.8	0.01	51.92	9.1
				II	19.8	−22	6.74	8445	32.2	27.45	0.7	62.63	61.68	0.01	51.84	9.1
Dittaino 1	48	4,152,373	477,907	2005	11.4	186.6	7.99	3230	18.65	12.44	0.66	28.45	23.64	0.47	28.52	6.7
Dittaino 2	49	4,147,461	483,150	2005	11.1	118.3	7.93	3430	19.96	13.45	0.62	31.42	27.34	0.48	31.6	7
Dittaino 3	50	4,141,538	486,604	2005	11	163	7.98	3390	18.24	12.41	0.59	30.62	25.93	0.6	27.5	6.5

I corresponds to August–October 2004 and II corresponds to April–May 2005

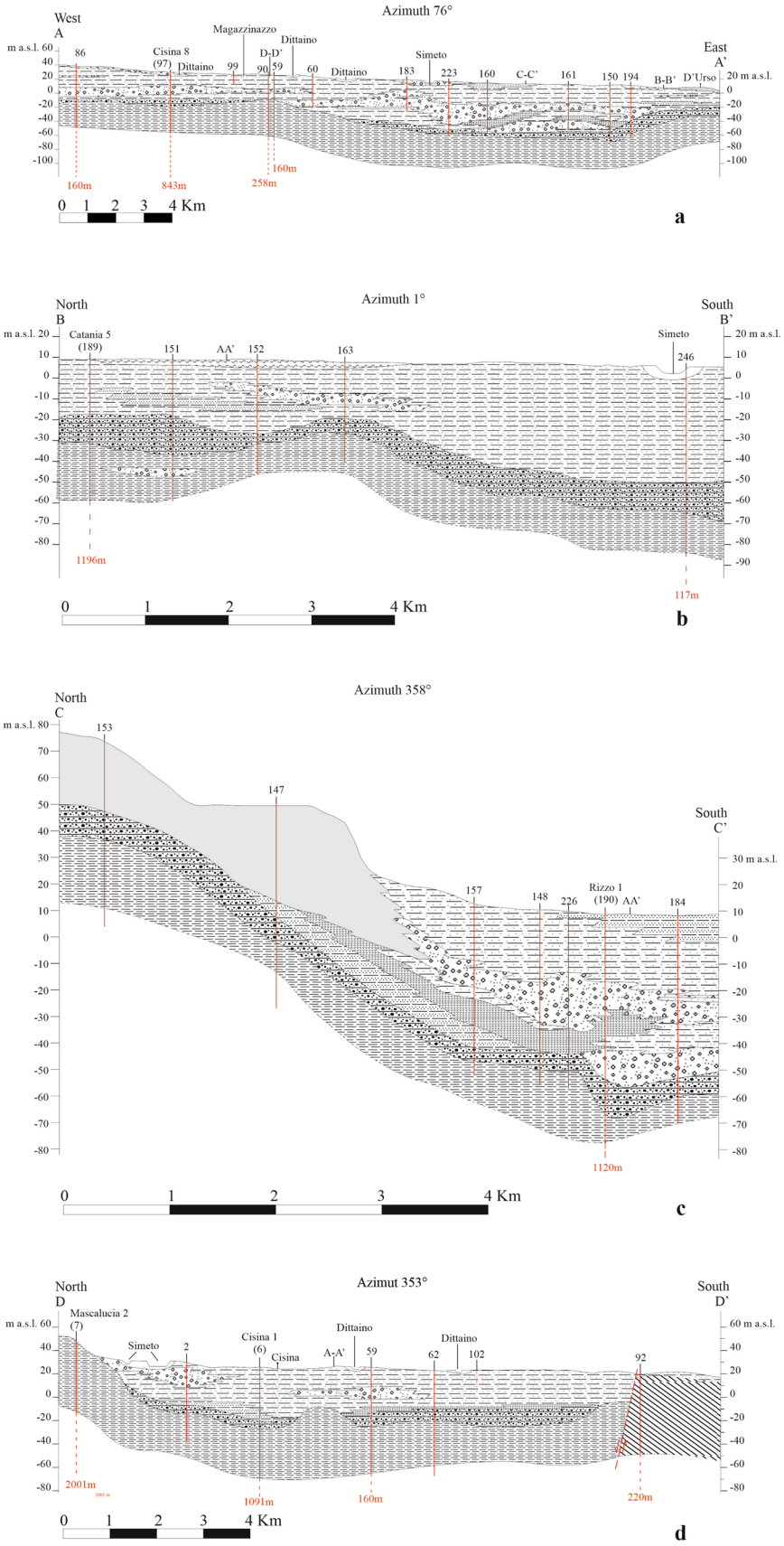

Fig. 3 Geological cross-sections as in Fig. 2: **a** A–A′ (azimuth near 76°); **b** B–B′ (azimuth near 1°); **c** C–C′ (azimuth near 358°); **d** D–D′ (azimuth near 353°). Cross-line sections and legend are in Fig. 1

Table 2 Hydrogeological scheme of the Catania Plain

Age	Lithology	Reservoir
Upper Pleistocene–Holocene	Alluvial-deltaic and coastal deposits	Shallow unconfined
Middle–Upper Pleistocene	Gravel with sandy conglomerate intercalations (Mt. Tiritì Formation)	Semi-confined
Middle Pleistocene	Sandstones and gravel (S. Giorgio Formation)	Semi-confined
Lower–Middle Pleistocene	Marine blue marly clay	Impermeable bedrock

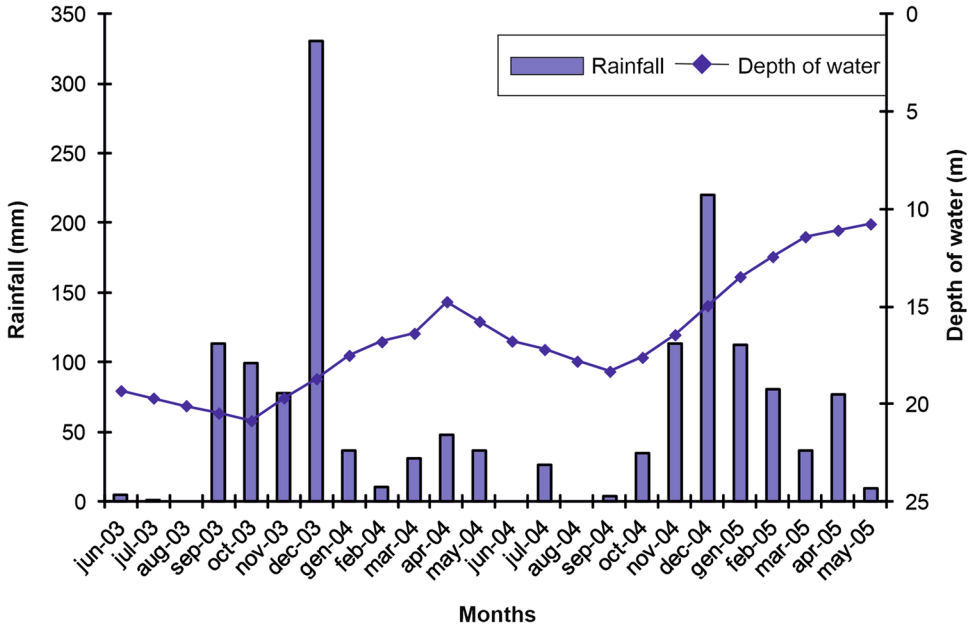

Fig. 4 Correlation between rainfall and groundwater level of Iunghetto phreatimeter

in the West–East direction, influencing the groundwater circulation.

Correlating the values of the piezometric level, recorded at the "Iunghetto" phreatimeter, (depth 52 m; Sicilian Regional Hydrographic Office) with our data of "Catania" rain gauge (Fig. 4), a statistical analysis was performed to calculate the lag time using cross-correlation. A groundwater "recharging delay" of about 4 months was obtained, defined as the time difference between the maximum rainfall and the consequent maximum groundwater level. This recharging delay is due to the pathway length of groundwater reaching the deepest aquifer.

Geochemical characterization of groundwater

The sampled waters show great variability in electrical conductivity ranging from 1000 to 10,500 µS/cm. Temperature values range from 15 to 33.5 °C with most of the samples showing slight differences between the two samplings. The pH values vary from slightly acidic (6.74, sample Zoo) to slightly basic (7.92, sample Sigona).

The representative hydrochemical classes of waters are Cl–SO_4–earth alkaline (75% of samples), Cl–SO_4–alkaline (17%) and bicarbonate–earth alkaline (8%) (Fig. 5).

In particular, two main assemblages can be recognized, one in the Tyrrhenian marine and continental alluvial sediments (group *b* in Fig. 5), and the other in the Holocene recent alluvial deposits (group *a* in Fig. 5), including the majority of sampled waters. Two minor groups include samples from the northern part (on the slope of Etna, group *c* in Fig. 5) and samples from the southern part (laying on Holocene alluvial deposits and Hyblean calcarenites and vulcanites, group *d* in Fig. 5) of the Plain.

Regarding group c, it is possible to assume a mixing with groundwater coming from Mt Etna characterized by high HCO_3^- concentration due to the interactions with magmatic CO_2 (Parello et al. 2001; Liotta et al. 2016).

The geochemical properties of groundwater are related to the drained lithological units and the mixing with natural waters of different origins (e.g., seawater, surface waters or other groundwater). Finally, these properties can hardly be altered by the presence of pollutants of anthropogenic origin.

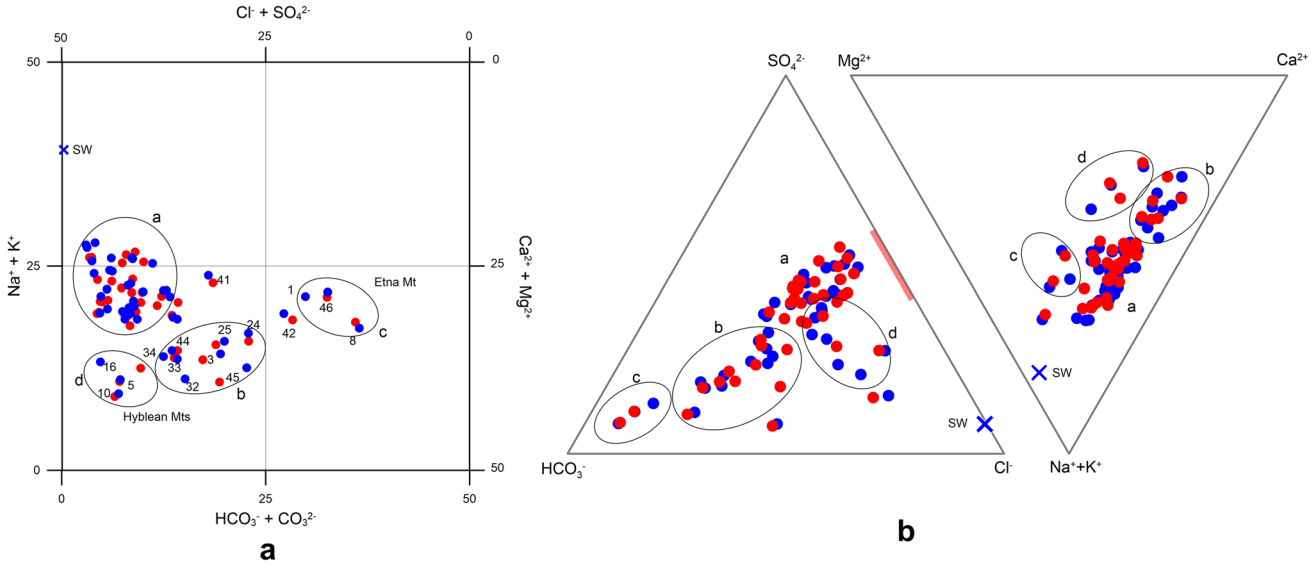

Fig. 5 **a** Square classification diagram of the investigated waters (after Langelier and Ludwig 1942). **b** Anion and cation triangular plot. Red bold line represents the SO_4^{2-}/Cl^- in the Etna plume. Blue circles represent first campaign, red circles second campaign. For groups a, b, c, d sees the text

In the plain, the contribution of seawater to the mixing processes, in areas near the coastline, is well known in the literature (Battaglia et al. 1991; Capaccioni et al. 2005). Seawater intrusion enhancement was attributed to the over-exploitation of deep wells located in correspondence with industrial areas (Battaglia et al. 1994; Capaccioni et al. 2005).

From the hydrogeological point of view, the groundwater of CP are fed by meteoric waters (rw), rivers and groundwater coming from Etna and Terreforti Hills reliefs to the North and Hyblean Mts to the South (Ferrara 1979).

The chemical composition of groundwater is strongly influenced by water–rock interaction. In particular, Ca^{2+} and Mg^{2+} (and $Na^+ + K^+$) can be originated by weathering of Silicate. In this case, the balance is controlled by HCO_3^- alone. An excess in HCO_3^- (Mg^{2+} and Ca^{2+} depletion) is indicative of silicate weathering or cation exchange reactions. In the studied area, few samples show this kind of behavior. More samples, on the contrary, show enrichment in Ca^{2+} or Mg^{2+}. Such enrichment in Ca^{2+} and Mg^{2+} over HCO_3^- and SO_4^{2-} may indicate reverse ionic exchange processes, very common in the interaction between groundwater and clays.

Our samples show, in some cases, an excess in $Na^+ + K^+$ with respect to Cl^- (Fig. 6), in other cases the opposite, further suggesting ion exchange reactions. In the cation exchange reaction, clays release Na^+ and K^+ to groundwater and adsorb Ca^{2+} and Mg^{2+}. In the reverse ion exchange, clays adsorb Na^+ and K^+ and release Ca^{2+} and Mg^{2+} in water according to the relation:

$$\text{Na}(\text{K}^+) - \text{Clay} + \text{Ca}^{2+}(\text{Mg}^{2+}) \Rightarrow 2\text{Na}^+(\text{K}^+) + \text{Ca}^{2+}(\text{Mg}^{2+})\ \text{Clay} \quad (1)$$

In Fig. 6, ion exchange processes are illustrated. The abscissa represents excess Na^+ and K^+ from sources other than halite dissolution, or seawater intrusion, and the ordinate represents Ca^{2+} and/or Mg^{2+} from processes unrelated to carbonate or gypsum dissolution. Water samples that are not altered by the above reactions are in the center (0, 0 coordinate) of the graph. The lower right corner of Fig. 6 indicates ion exchange occurring according to Eq. (1), (Na^+ would be high and Ca^{2+} would be low), while the upper left corner may be due to reverse ion exchange or other processes.

Looking at the geographic distribution of the EC (Fig. 7b), it is evident that seawater is probably not the cause of high ion concentrations in the water samples.

In fact, the Na^+/Cl^- ratios in groundwater with high ionic concentrations differ from the ratio of the sea, being closer to the 1/1 ratio of halite (Fig. 7c). Furthermore, as evidenced in Fig. 7d, the concentrations of Ca^{2+} and Mg^{2+} at the sampled sites rule out contamination due to marine ingression.

In particular, the highest EC and Na^+ and Cl^- concentrations (but also of other major constituents, Table 1) are located in the central part of the Plain. Moreover, they show an opposite trend from the coastline to the inner of the Plain and in particular along the Dittaino river banks (Fig. 7a, b)

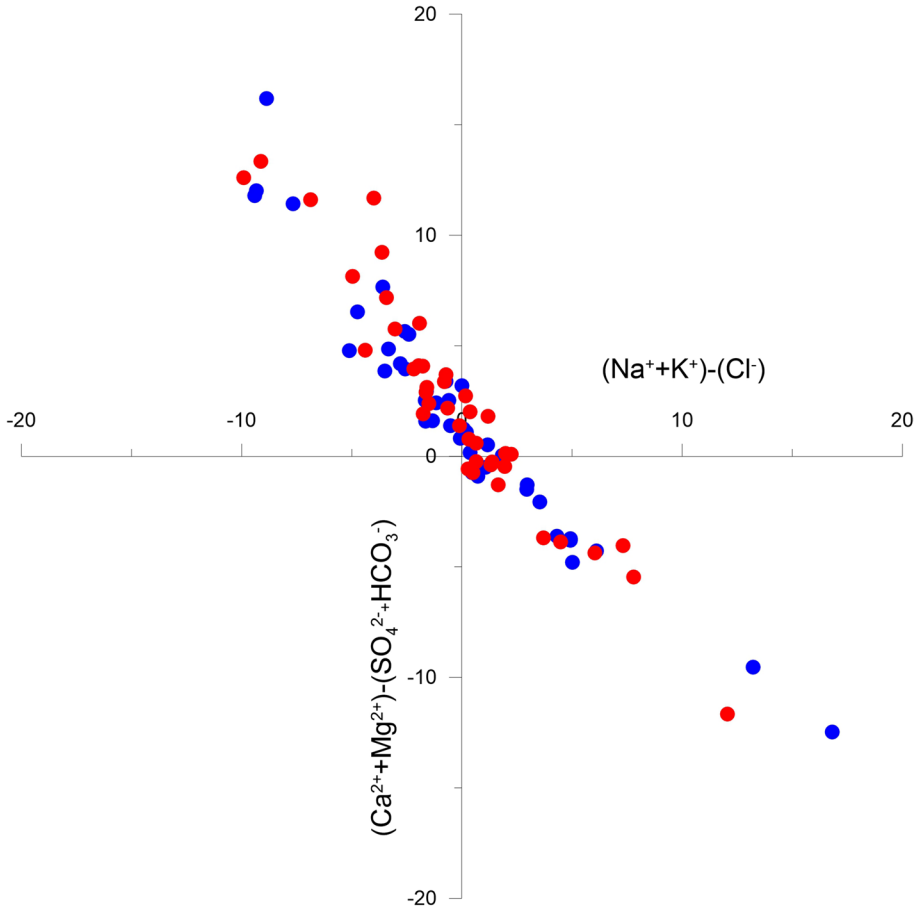

Fig. 6 Relationship between $(Ca^{2+}+Mg^{2+})$–$(HCO_3^-+SO_4^{2-})$ and (Na^++K^+)–(Cl^-) reflecting the cation exchange processes. The deficit or excess of (Na^++K^+) over Cl^- ions is compensated by the corresponding changes of $(Ca^{2+}+Mg^{2+})$ over the $(HCO_3^-+SO_4^{2-})$ ions. Blue circles represent first campaign samples, red circles represent second campaign samples

and in the proximity of farms. Direct involvement of Dittaino water in these high EC values can be excluded due to its relatively low EC (< 3000 µS/cm) with respect to the anomalous areas (Table 1). Samples taken at sites near streams show higher SO_4^{2-}, Na^+ and Cl^- contents, respectively, due to the interaction of surface water with evaporite lithologies (Gessoso Solfifera formation).

Almost all samples on the western side of the plain show a Ca^{2+}/SO_4^{2-} ratio typical of gypsum dissolution. Gypsum outcrops occur only in a very little portion of the NNW of the plain. Due to the W–E flow direction, it is possible to hypothesize a mixing with groundwater coming from the area at the west of the plain, where gypsum is present (Gessoso Solfifera formation).

Water–rock interaction phenomena can strongly affect groundwater chemistry and therefore Ca^{2+}, Mg^{2+} and HCO_3^- can be originated from carbonate rock dissolution and Ca^{2+} and SO_4^{2-} from gypsum and anhydrite. In the latter case, samples should plot on or close to the 1:1 ratio line (Fig. 8a).

Battaglia et al. (1994) supposed a sulfate origin associated with shallow biochemical reactions. Moreover, as observed by Aiuppa et al. (2001) and Liotta et al. (2016), the composition of meteoric waters in the southern side of Mt Etna, is enriched in Cl^- and SO_4^{2-} due to interaction with the plume, influencing the composition of groundwater (Fig. 5b). Instead, the high concentrations of SO_4^{2-} shown in Fig. 8a (yellow area) compared with Ca^{2+} concentrations are probably due to depletion in Ca^{2+} consequent to the precipitation of calcium carbonate minerals. Indeed, almost all the samples are oversaturated in calcite, dolomite and aragonite (SI > 1), while they are undersaturated with respect to gypsum and anhydrite. Only the westernmost samples are almost saturated with gypsum, so a dissolution of this solid phase can be assumed. It is therefore possible to hypothesize that the input of gypsum-derived Ca^{2+} induces the oversaturation of carbonate minerals and the consequent precipitation of Ca^{2+} and possibly Mg^{2+} in the form of Calcite and Dolomite (Fig. 8b, c). This could explain the high concentrations of SO_4^{2-} in solution and a SO_4^{2+}/Ca^{2+} ratio higher than 1 in most sulfate-rich waters (Fig. 8a).

The rather uniform behavior of all investigated parameters during wet and dry sampling periods could indicate the stability in the "non-punctual contaminant source" (natural or anthropogenic). In contrast, a clear "punctual pollutant source" could be identified in the Bernardello, Magazzinazzo and Panni samples, where large differences in NO_3^- concentrations are observed between the two

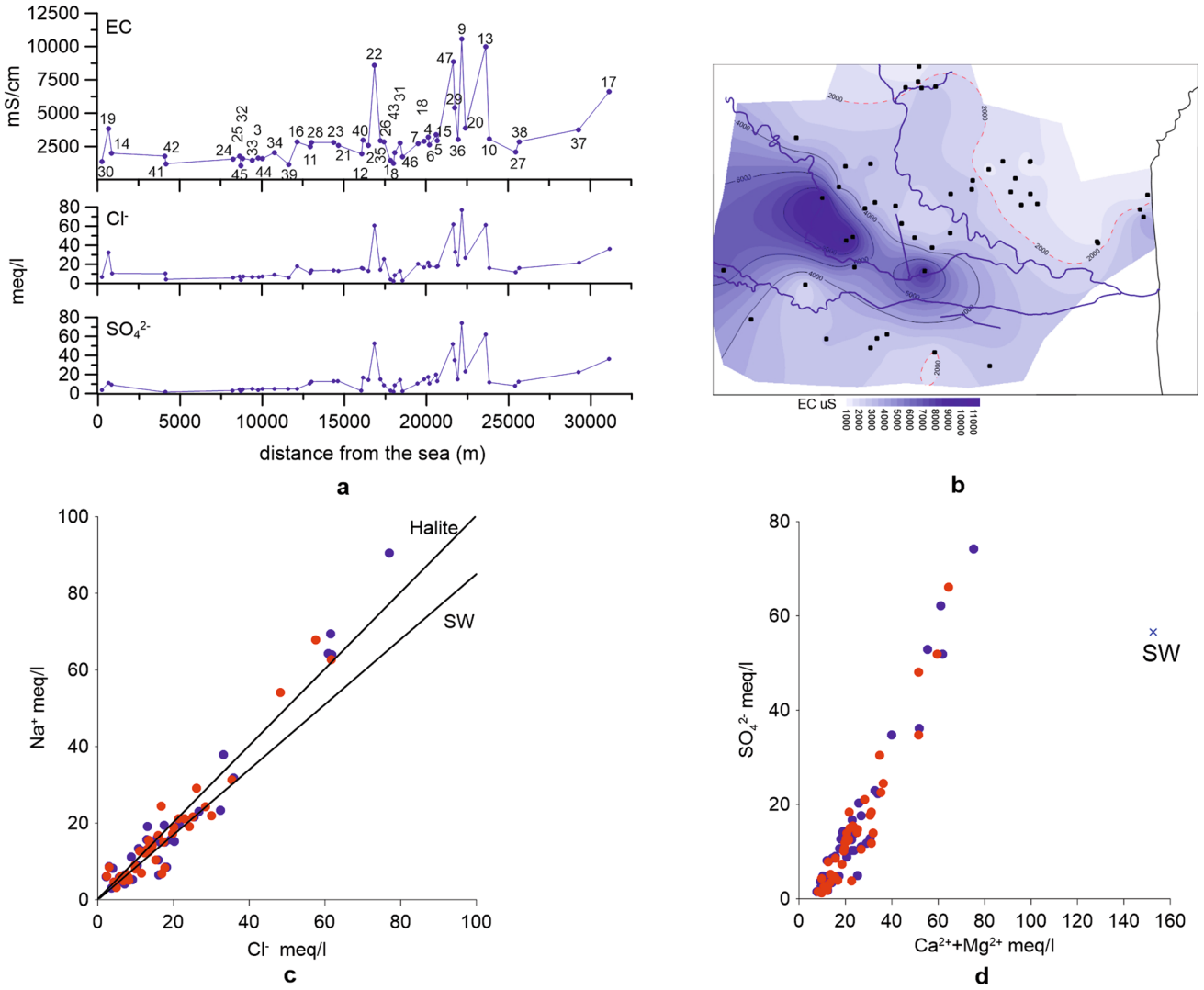

Fig. 7 **a** Electric conductivity (EC in µS/cm), Cl^- and SO_4^{2-} concentrations vs distance to the cost line. **b** Electric conductivity (EC in µS/cm) distribution map during the first sampling campaign. **c** Sodium vs chloride concentration in the sampled waters. **d** Calcium + magnesium vs sulfate concentration in the sampled waters. Blue circles represent first campaign samples, red circles represent second campaign samples

samplings. Nitrogen-based fertilization, of the extensive citrus groves in the CP, is carried out in the spring period. The difference in concentration of elements, normally used in agriculture as fertilizer (K^+, NO_3^-, SO_4^{2-} rich), suggests pollution linked to this kind of land use (Amano et al. 2016).

In almost all samples, NO_3^- concentrations exceed the WHO limit (50 mg/l) for drinking water. The highest concentrations are found in D'Agati (> 300 mg/l) and Galermo (> 400 mg/l) samples. In the central part of the CP, nitrate pollution is under the WHO limit. Sulfate does not follow the same distribution as NO_3^-. The more intense NO_3^- polluted areas do not coincide with the more elevated SO_4^{2-} concentrations. The cause of that difference is the multiple origins of sulfate in CP: one, natural coming from both the Gessoso Solfifera evaporites and the Etna plume, and the other anthropogenic, according to Ferrara (1999), coming from agriculture.

Isotopic composition of groundwater

The isotopic composition of groundwater is a useful tool to comprehend the main physical processes leading to its origin (meteoric, marine and/or mixing with other groundwater) and to recognize water–rock interaction phenomena. If the isotopic composition of local rainwater is known, it is possible to identify approximately the source (altitude) and pathway of groundwater recharge. The lack of important reliefs inside the plain and the presence of Mt. Etna to the North and Hyblean Mts to the South affect

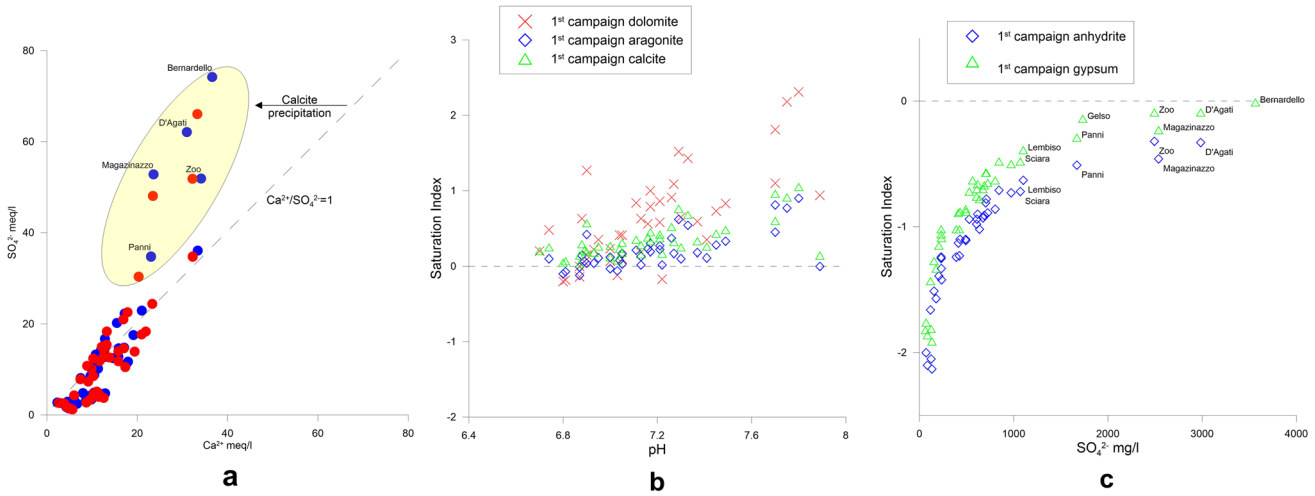

Fig. 8 **a** Calcium vs sulfate in the sampled waters. The straight line represents $Ca^{2+}/SO_4^{-}=1$. Blue circles represent first campaign samples, red circles represent second campaign samples. **b** Saturation index of calcite, aragonite and dolomite in sampled waters. **c** Saturation index of anhydrite and gypsum in sampled waters

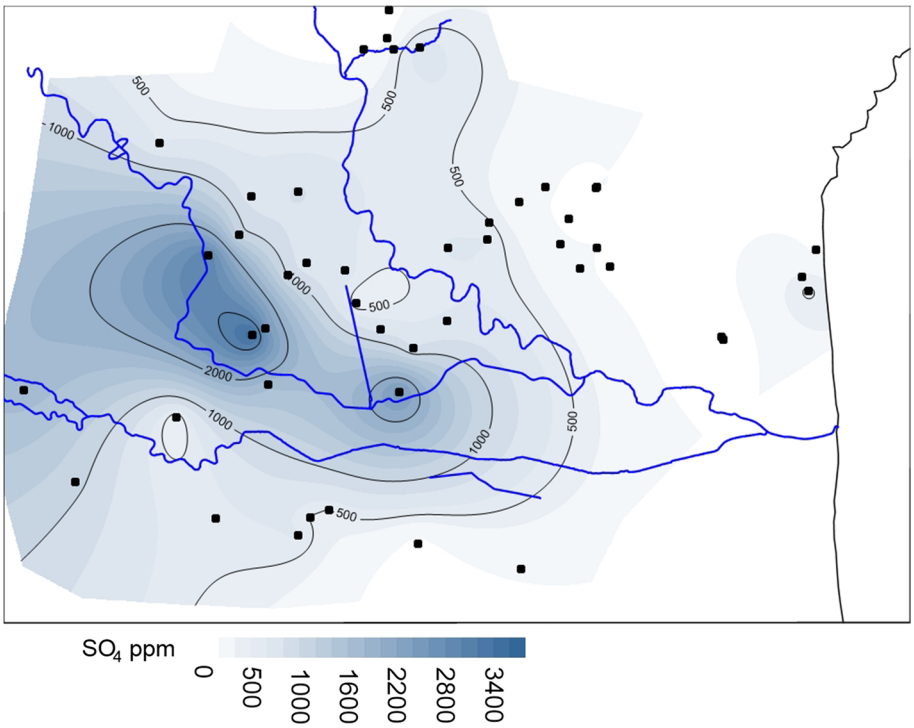

Fig. 9 Distribution map of SO_4^{2-} during the first sampling survey

the isotopic composition of the meteoric water about to the origin of the air masses. Mt. Etna (3320 m asl) has climatic conditions different with respect to the surrounding areas and it is characterized by more negative δ^2H and $\delta^{18}O$ values than the rest of Sicily (δ^2H −43‰ and $\delta^{18}O$ −7.00‰, D'Alessandro et al. 2004; Liotta et al. 2013). Due to its altitude, it represents a morphological barrier for clouds and rain and induces an isotopic fractionation (more negative δ^2H and $\delta^{18}O$ values) of rainwater coming from its northern and eastern sectors. On the contrary, the Hyblean plateau is characterized by low rainfall compared to the northern areas of Sicily and by the highest average values of the annual temperatures. The isotopic composition of rainwater coming from the Hyblean plateau is more positive also due to evaporation during rainfall or runoff (Grassa et al. 2006) (Fig. 9).

The most negative values of the rainwater collected in the study area were recorded in the winter with a minimum

Table 3 Description of the monthly values and weighted mean of the δ^2H and $\delta^{18}O$ (‰) isotopic composition of rain water

Name			Pl Scordia			Pl Catania			Pl Ramacca
Elevation m asl			158			200			285
Latitude N UTM			4,127,555			4,153,726			4,137,764
Longitude E UTM			485,847			506,411			473,149
Distance from sea			23 km			3.5 km			35 km
Months	δ^2H	$\delta^{18}O$	P mm	δ^2H	$\delta^{18}O$	P mm	δ^2H	$\delta^{18}O$	P mm
Jun 2004	N.D	N.D	0	N.D	N.D	0	3	−0.43	3.11
Jul 2004	−15	−3.69	6.37	−16	−3.35	27.3	N.D	N.D	0
Aug 2004	N.D	N.D	0	N.D	N.D	0	−7	−2.98	12.87
Sep 2004	−31	−5.47	57.58	1	−0.64	4.24	−25	−4.45	24.76
Oct 2004	−32	−4.5	13.72	−18	−3.61	36.92	−21	−4.18	49.09
Nov-04	−31	−5.6	162.27	−37	−6.47	119.54	−34	−6.74	161.98
Dec 2004	−31	−5.76	199.33	−30	−5.91	232.01	−35	−6.7	140.34
Jan 2005	−57	−9.22	51.64	−39	−7.26	118.13	N.D	N.D	N.D
Feb-05	−30	−6.77	125.91	−39	−7.34	84.88	−69	−6.76	55.46
Mar-05	−18	−4.9	65.08	−34	−7.15	38.2	−69	−10.72	103.98
Apr-05	−36	−5.8	33.25	−31	−6.05	81.35	−22	−5.5	61.26
May 2005	−24	−3.79	7.92	−30	−4.66	9.9	−38	−6.6	20.94
Weighted mean	−32	−5.98		−32	−6.16		−40	−6.87	

ND not detected

value of −10.7‰ and −69‰ for $\delta^{18}O$ and δ^2H, respectively, while the most positive values (−0.43‰ for $\delta^{18}O$ and + 3‰ for δ^2H) were observed in the summer season (Table 3).

The variability in the isotopic composition of precipitation reflects the seasonal variation in air temperature. Figure 10a shows the monthly δ^2H and $\delta^{18}O$ isotopic composition of rainfall for the 2004/2005 hydrological year. The Global Meteoric Water Line (GMWL; Craig 1961) and the Eastern Mediterranean Meteoric Water Line (EMMWL; Gat and Carmi 1970) are plotted for comparison. Based on the weighted mean of the δ^2H and $\delta^{18}O$ (‰) isotopic composition of rainwater (Table 3), the Local Meteoric Water Line ($\delta^2H = 6.47\ \delta^{18}O + 6.37$; LMWL) was determined. The slope (6.4) of the LMWL, lower than that of the GMWL and EMMWL, indicates that precipitations on the CP have a predominantly local origin (Liotta et al. 2008) suggesting the occurrence of raindrops re-evaporation processes. The deuterium excess parameter *d* was computed according to Dansgaard's (1964) definition $d = \delta^2H - 8\ \delta^{18}O$. The estimated deuterium excess value ($d = +16$‰) is typical of the western Mediterranean regions (Celle 2000) where, moisture derives from prevailing disturbances from eastern Mediterranean (*d*-excess = + 22‰ Gat and Carmi 1970) to North Atlantic (*d*-excess = + 10‰ Craig 1961) provenance. An average *d*-excess value of + 14‰ was assumed to be a regional isotope signature of precipitation in the western Mediterranean (Celle 2000).

Groundwater samples (Fig. 10b) fall on the LMWL line indicating a predominantly meteoric origin. The slope of the groundwater line (not shows in Fig. 10) is less than that of rainwater, suggesting evaporation before its infiltration into the subsoil.

The recharge areas of the CP groundwater were identified from the estimation of the vertical isotopic gradient (Fig. 10c). In Fig. 10c, it was possible to recognize three groups of water. The groundwater belonging to group 1, (similar to group c of Fig. 5), in which samples located in the northern area of the plain are grouped, are characterized by the most negative values of $\delta^{18}O$ and δ^2H (Auto, $\delta^2H = -43$‰ and $\delta^{18}O = -7.13$‰; Walker, $\delta^2H = -43$‰ and $\delta^{18}O = -7.05$‰, see Table 3) typical of high altitude recharge areas. This deviation can be related to interactions/mixing with aquifers coming from the Etnean area, fed by heights compatible with those obtained from the graph in Fig. 10c (D'Alessandro et al. 2004; Liotta et al. 2013). On the contrary, group 2 (similar to group d of Fig. 5), consisting of the sampling points located in the southern area of the CP, shows more positive isotopic values compared to the isotopic gradient related to their position (Arcimusa, $\delta^2H = -25$‰ and $\delta^{18}O = -3.81$‰; Arcimusa 2, $\delta^2H = -25$‰ and $\delta^{18}O = -4.13$‰; Arcimusa 3, $\delta^2H = -26$‰ and $\delta^{18}O = -4.24$‰; Chiesa, $\delta^2H = -28$‰ and $\delta^{18}O = -4.50$‰, see Table 3). This characteristic may be due to secondary evaporative processes or to the exploitation of groundwater from the northern flank of Hyblean Mts,

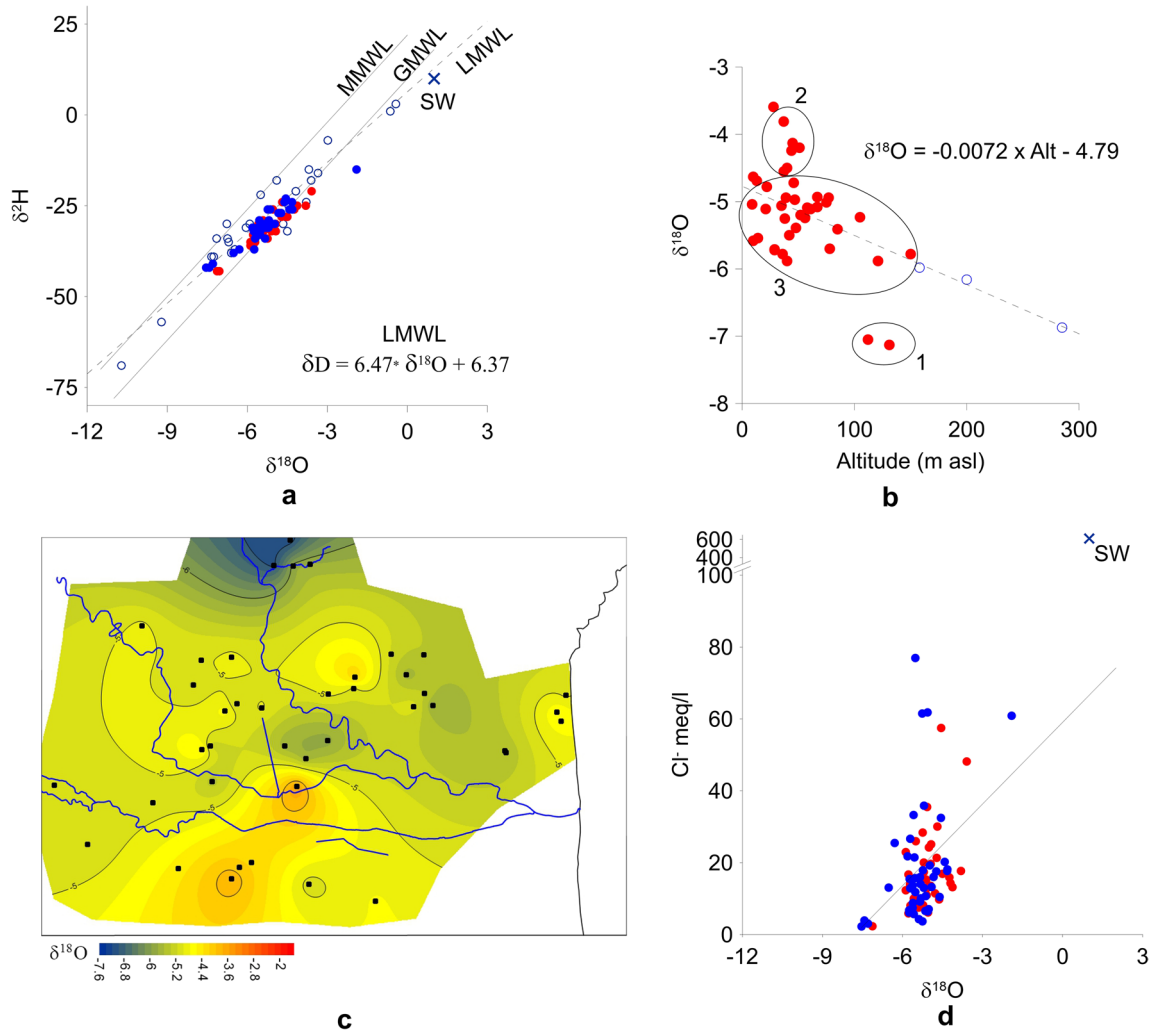

Fig. 10 **a** Plots of $\delta^{18}O‰$ vs. $\delta^{2}H$ of rainwaters and sampled groundwater. *LMWL* local meteoric water line; *GMWL* global meteoric water line; *MMWL* Mediterranean meteoric water line; empty blue circles represent monthly isotopic values rain waters; data from Tables 3 and 4. **b** Plots of groundwater $\delta^{18}O‰$ vs. altitude; empty blue circles represent weighted $\delta^{18}O‰$ rain water (June 2004–May 2005); data from Tables 3 and 4. **c** Distribution map of $\delta^{18}O‰$ of groundwater during the second campaign. **d** Plots of $\delta^{18}O‰$ vs Cl^{-} of groundwater. Full blue circles represent first campaign groundwater, full red circles represent second campaign groundwater

characterized, as mentioned above, by more positive isotopic values (Fig. 10e). The most positive values of the Magazinazzo sample ($\delta^{2}H = -15‰$ and $\delta^{18}O = -1.91‰$, tab. 3) are instead related to evaporation processes inside the well, caused by the large diameter of the well itself. Finally, group 3 (similar to groups a and b of Fig. 5), represented by waters located in the central area of the plain whose average altitude is about 50 m asl, shows values of $\delta^{18}O$ perfectly aligned with the vertical isotopic gradient calculated for the area of the CP. The aquifers belonging to this group are, therefore, fed by precipitations that fall within the area of the CP (Table 4).

Furthermore, the relationship between $\delta^{18}O‰$ and the concentration of Cl^{-} (Fig. 10d) excludes a marine intrusion into the surface water of the CP.

Conclusions

Based on our elaborations and previous data (Ferrara 1999), it was possible to define typology, boundaries, geometry and a water circulation model of the study aquifer.

Present and recent alluvial deposits, continental and marine alluvial terraces and sands, sandstones and conglomerates of Medium–Upper Pleistocene with heterogeneous granulometry, 80–100 m in maximum thickness, constitute the alluvial aquifer. It is characterized by highly variable horizontal and vertical porosity, permeability (5×10^{-2} m/s ÷ 10^{-4} m/s) and transmissivity (1×10^{-3} $m^2/s \div 5 \times 10^{-3}$ m^2/s) influencing water flow inside the

Table 4 Descriptive of the isotopic δ^2H and $\delta^{18}O$ (‰ vs SMOW) composition of the groundwater

Name	Elevation m asl	δ^2H (I)	$\delta^{18}O$ (I)	δ^2H (II)	$\delta^{18}O$ (II)
3 Fontane	120	−42	−7.43	N.S	N.S
Agnelleria	150	−38	−6.52	−36	−5.78
Alcalà	78	−34	−5.75	−33	−5.7
Archi	67	−31	−5.81	−32	−4.93
Arcimusa	37	−26	−4.32	−25	−3.81
Arcimusa 2	45	−24	−4.33	−25	−4.13
Arcimusa 3	44	−26	−4.42	−26	−4.24
Auto	131	−42	−7.54	−43	−7.13
Bernardello	37	−31	−5.52	−28	−4.55
Chiesa	40	−27	−4.83	−28	−4.5
Chiesa 2	51	−32	−5.13	−32	−4.2
Cisina	29	−37	−5.74	−35	−5.72
D'Agati	43	−31	−5.26	N.S	N.S
D'Urso	13	−23	−4.56	−24	−4.69
Fondo	46	−27	−4.74	−28	−4.72
Galermo	22	−26	−5.23	−27	−4.78
Gelso	67	−29	−5.19	−30	−5.08
Gerbini	52	N.D	−5.28	−31	−5.2
Grimaldi	10	−24	−4.61	−24	−4.63
Lembiso	56	−32	−5.71	−34	−5.24
Maddalena	40	−34	−5.71	−35	−5.88
Magazinazzo	28	−15	−1.91	−21	−3.59
Mazza	39	−33	−5.62	−30	−4.94
Messina1	36	−32	−5.58	−33	−5.78
Messina2	48	−33	−5.67	−32	−5.39
Oleificio	121	−37	−6.3	−36	−5.88
Ovo	58	−32	−5.52	−32	−5.09
Palazzello	35	−32	−4.91	−30	−5.06
Panni	42	−32	−5.59	−32	−5.5
Paternò	9	−26	−5.14	−26	−5.04
Portiere Stella	47	−31	−5.21	−30	−4.97
Rinazzi	92	−30	−5.02	N.S	N.S
San Martino	61	−32	−5.05	−31	−5.11
Santa Lucia	105	−33	−5.34	−31	−5.23
Santonocito	29	−34	−5.33	−35	−5.71
Sarpietro	75	−30	−4.98	−31	−5.01
Sciara	55	−29	−5.55	−31	−5.2
Sferro	77	−33	−5.52	−30	−4.94
Sfondato	85	−32	−5.76	N.S	N.S
Sigona	21	−30	−5.35	−30	−5.11
Sole1	10	−31	−5.31	−30	−5.58
Sole2	14	−31	−5.39	−30	−5.54
Stella	32	−32	−5.61	N.S	N.S
Terre Bianche	74	−31	−5.62	N.S	N.S
Vivaio	85	−30	−5.25	−29	−5.41
Walker	112	−41	−7.29	−43	−7.05
Zoo	38	−30	−5.06	−30	−5.25

ND not detected; *NS* not sampled

aquifer (Ferrara 1999; Ferrara and Pappalardo 2004). The low permeability in recent alluvial deposits creates a decrease in the interconnection between deposits and, as a consequence, the creation of an alluvial multilayered aquifer formation. The blue Marly-clays (Low Pleistocene) constitute its impermeable substratum.

The aquifer is fed by both rainfall and sub-river bed aquifers draining the waters of the Dittaino, Gornalunga and Simeto Rivers. The main flow direction of groundwater in the area is W-E following that of the hydrographic network (Ferrara 1999). In agreement with Ferrara, the cross-section of Fig. 3a shows the morphology of the top of the confining clayey bed characterized by many depressions roughly trending in the West–East direction, influencing the groundwater circulation.

In the North, close to Mt Etna, the shallower aquifer, laid in the marine and continental alluvial terracing, a hydraulic connection exists with both the Etnean aquifer and the intermediate and deep alluvial aquifers as hypothesized by Ferrara (1999) and Capaccioni et al. (2005) and confirmed by the present chemical and isotopic analyses.

Also in the south, there are hydraulic connections between the alluvial aquifer of the CP and the Hyblean aquifer, although limited by the presence of dense and uninterrupted clayey and clayey-sandy levels that partially obstruct the water flow.

Based on our pluviometric data and freatimetric data from the literature (Sicilia Regional Hydrographic Office) an aquifer recharge lag time of about 4 months was estimated.

From (i) geological and hydrogeological considerations and (ii) chemical and isotopic compositions of groundwater, the first model of groundwater circulation of the entire plain has been developed. In particular, it was possible to define the alluvial multilayer aquifer consisting of a shallow unconfined, an intermediate semi-confined and a deep semi-confined aquifer.

Four chemical assemblages have been recognized in CP water samples. Two major assemblages refer to waters circulating in (i) the Holocene recent alluvial deposits (identified as group a), comprehending the majority of sampled waters, and (ii) the Tyrrhenian marine and continental alluvial (identified as group b). Two minor groups comprehending samples (iii) near the southern slope of Etna (identified as group c) and (iv) on the north of the Hyblean plateau laying

on Holocene alluvial deposits and Hyblean calcarenites and vulcanites (identified as group d).

The processes characterizing the CP water compositions are related to interactions with clay lithology present in the Plain and/or sediments of the Gessoso Solfifera series, outcropping in the reliefs located in the West of the area under study. This assumption is supported by the West–East flow direction of groundwater (Ferrara 1999). In addition, Mt. Etna plays a significant role in the composition of groundwater in North of the Plain. For example, the presence of sulfates can be due to the interaction between local meteoric waters feeding groundwater and the Etna plume. The dissolution of CO_2 of magmatic origin in the groundwater justify the high content of bicarbonates.

The marine intrusion, highlighted near the coastal area in previous studies (Ferrara 1999; Battaglia et al. 1991; Capaccioni et al. 2005), is not observed in our samples. The reason for that behavior is that the wedge of marine intrusion, caused by the over-exploitation of the aquifer, affects mainly the deeper aquifers and is limited to areas close to the coast, only partially investigated in this research.

Sulfate enrichment, especially in the western area of the CP, derives from the dissolution of evaporitic deposits of the Gessoso Solfifera Formation outcropping to the west of the CP. The SO_4^{2+}/Ca^{2+} ratios higher than that of gypsum are caused by calcite precipitation. The high concentrations of chlorides, nitrates, sulfates and potassium in some samples, are also linked to the anthropogenic pollution produced by the intense agricultural (use of fertilizers, pesticides) and zootechnical activity as well as by a large industrial area (industrial waste). EC values and major ion concentrations show a systematic control of land use characteristics and tend to increase mainly toward the biggest farms and zootechnics. Therefore, their distribution of them reflects the dominant land use around each well and indicates the effects of anthropogenic contamination.

Based on the isotopic composition of water, in the same way as evidenced by the chemical composition, it was possible to distinguish three refill areas of the CP aquifer. One, on the North, was attributable to Mount Etna and is characterized by mean meteoric recharge altitudes over 800 m asl, one on the South-West, is ascribed to the medium altitude Hyblean plateau and the hills around it and the third, in the central part of the CP, is ascribed to the local recharge of the CP (< 100 m asl).

Acknowledgements Thanks are due to the working group of INGV, Sezione di Palermo for the sampling and analyses of groundwater. We kindly acknowledge the comments and suggestions of Walter D'Alessandro on a previous version of the manuscript.

Author contributions All the authors contributed to the study's conception and design. Material preparation, data collection and analysis were performed by SM, LLP, EGC, RF, CS and GP. SM, GP and LLP wrote the first draft of the manuscript and all the authors commented on previous versions of the manuscript. All the authors read and approved the final manuscript.

Funding Open access funding provided by Istituto Nazionale di Geofisica e Vulcanologia within the CRUI-CARE Agreement. This research was funded and commissioned by Regione Siciliana, Commissario Delegato per l'Emergenza Bonifiche e la Tutela delle Acque in Sicilia to Istituto Nazionale di Geofisica e Vulcanologia-Sezione di Palermo for the redaction of the Piano di Tutela delle Acque della Sicilia (2007).

Data availability Geochemical data generated or analyzed during this study are included in the published article. The remaining data will be made available on request.

Declarations

Conflict of interest The authors declare no conflict of interest. The funders had no role in the design of the study, in the collection, analyses, or interpretation of the data, in the writing of the manuscript, or in the decision to publish the results.

References

Aiuppa A, Bonfanti P, Brusca L, D'Alessandro W, Federico C, Parello F (2001) Evaluation of the environmental impact of volcanic emissions from the chemistry of rainwater: Mount Etna area (Sicily). Appl Geochem 16:985–1000. https://doi.org/10.1016/S0883-2927(00)00075-5

Amano H, Nakagawa K, Berndtsson R (2016) Groundwater geochemistry of a nitrate-contaminated agricultural site. Environ Earth Sci 75:1145. https://doi.org/10.1007/s12665-016-5968-8

Battaglia M, Cimino A, Dongarrà G, Gottini V, Hauser S, Rizzo S (1991) Hydrogeological and chemical outlines of the margin area Palagonia-Lentini-Augusta (South-Eastern Sicily). Mem Soc Geol Ital 47:567–573

Battaglia M, Bonfanti P, Gottini V, Rizzo S (1994) Distribuzione degli elementi maggiori minori ed in traccia nelle acque sotterranee della piana costiera di Catania (Sicilia SE). Acqe Sotterranee 46:17–29

Breusse JJ, Huot G (1954) Hydrogeological surveys in the Catania area by means of electrical soundings. Geophys Prospect. https://doi.org/10.1111/j.1365-2478.1954.tb01288.x

Capaccioni B, Didero M, Paletta C, Didero L (2005) Saline intrusion and refreshening in a multilayer coastal aquifer in the Catania Plain (Sicily, Southern Italy): dynamics of degradation processes according to the hydrochemical characteristics of groundwaters. J Hydrol 307:1–16. https://doi.org/10.1016/j.jhydrol.2004.08.037

Cassa per il mezzogiorno (1982) Indagini idrogeologiche e geofisiche per il reperimento di acque sotterranee per l'approvvigionamento idrico del sistema V zona centro orientale della Sicilia (catanese)

Catalano R, Franchino A, Merlini S, Sulli A (2000) Central Western Sicily structural setting interpreted from seismic reflection profiles. Mem Soc Geol Ital 55:5–16

Catalano S, Monaco C, Tortorici L, Paltrinieri W, Steel N (2004) Neogene-quaternary tectonic evolution of the southern Apennines. Tectonics. https://doi.org/10.1029/2003TC001512

Celle H (2000) Caractèrisation des prècipitations sur le pourtour de la Mèditerranèe occidentale. Approche isotopique et chimique, thesis, Universit6 Avignon, 2000

Craig H (1961) Isotopic variations in meteoric waters. Science 133:1702–1703

D'Alessandro W, Federico C, Longo M, Parello F (2004) Oxygen isotope composition of natural waters in the Mt. Etna area. J Hydrol 296:282–299

Dansgaard W (1964) Stable isotopes in precipitation. Tellus 16:436–468

Ferrara V (1979) Risultati preliminari delle ricerche idrogeologiche e geochimiche eseguite nell'area della provincia di Catania. Atti 1° Sem. inf.Un. Ric. Sottoprogetto "Energia geotermica". CNR-PF Energetica, Roma 18–21 dicembre 1979, pp 549–555

Ferrara V (1998) Sintesi dei risultati delle ricerche sugli acquiferi della Piana di Catania (Sicilia Orientale). Atti giornata mondiale dell'acqua, "Acque sotterranee: Riorsa Invisibile". ICIC-CIID, GNDCI-CNR, Roma

Ferrara V (1999) Presentazione della carta di vulnerabilità all'inquinamento dell'acquifero alluvionale della Piana di Catania (Sicilia NE). Atti del 3° Conv. Naz. Sulla protezione e Gestione delle Acque Sotterranee per III Millennio. Parma, 13–14–15 ottobre 1999

Ferrara V, Marchese G (1977) Ricerche idrogeologiche su alcuni acquiferi alluvionali della Sicilia orientale. Atti Acc Gioenia Sc Nat S VII 9:189–230

Ferrara V, Pappalardo G (2004) Intensive exploitation effects on alluvial aquifer of the Catania plain, Eastern Sicily, Italy. Geofís Int 43:671–681

Gat JR, Carmi I (1970) Evolution of isotopic of atmospheric waters in the Mediterranean Sea area. J Geophys Res 75:1437–1440

Grasso M, La Manna F (1990) Lineamenti stratigrafici e strutturali del fronte della falda di Gela affiorante a NW del plateau ibleo (Sicilia Sud-orientale). Geologica romana, pp 55–72

Grassa F, Favara R, Valenza M (2006) Moisture source in the Hyblean Mountains region (southeastern Sicily, Italy): evidence from stable isotopes signature. Appl Geochem 21:2082–2095. https://doi.org/10.1016/j.apgeochem.2006.07.014

Guastaldi E, Carloni A, Pappalardo G, Nevini J (2014) Geostatistical methods for lithological aquifer characterization and groundwater flow modeling of the Catania plain quaternary aquifer (Italy). J Water Res Protect 6:272–296

INGV-Regione Siciliana, Piano di Tutela delle Acque della Regione Sicilia (2005) Prima caratterizzazione e monitoraggio delle Acque Sotterranee finalizzata alla redazione del "Piano di Tutela delle Acque della Regione Sicilia". Commissario Delegato per l'Emergenza Rifiuti e Tutela delle Acque

Lentini F (1982) The geology of the Mt. Etna basement. Mem Soc Geol Ital 23:7–25

Liotta M, Bellissimo S, Favara R, Valenza M (2008) Isotopic composition of single rain events in the central Mediterranean. J Geoph Res 113:D16304. https://doi.org/10.1029/2008JD009996

Liotta M, Grassa F, D'Alessandro W, Favara R, Gagliano Candela E, Pisciotta A, Scaletta C (2013) Isotopic composition of precipitation and groundwater in Sicily, Italy. Appl Geochem 34:199–206. https://doi.org/10.1016/j.apgeochem.2013.03.012

Liotta M, D'Alessandro W, Bellomo S, Brusca L (2016) Volcanic plume fingerprint in the groundwater of a persistently degassing basaltic volcano: Mt. Etna. Chem Geol 433:68–80. https://doi.org/10.1016/j.chemgeo.2016.03.032

Parello F, D'Alessandro W, Aiuppa A, Federico C (2001) Cartografia geochimica degli acquiferi etnei. Gruppo Naz. per la Difesa dalle Catastrofi Idrogeologiche del CNR-pubbl. n. 2190. Officine Grafiche Riunite Palermo

Torelli L, Grasso M, Mazzoldi G, Peis D (1998) Plio-Quaternary tectonic evolution and structure of the Catania foredeep, the northern Hyblean Plateau and the Ionian shelf (SE Sicily). Tectonophysics 298(1):209–221. https://doi.org/10.1016/S0040-1951(98)00185-1